Quantification of myocardial perfusion using dynamic CT perfusion analysis on third generation dual source CT in an ex-vivo porcine heart model

Award:	Magna Cum Laude
Poster No.:	P-0040
Congress:	ESCR 2016
Type:	Scientific Poster
Authors:	G. J. Pelgrim[1], T. duguay[2], M. Stijnen[3], A. Varga-Szemes[4], S. Van Tuijl[3], U. J. Schoepf[4], M. Oudkerk[1], R. Vliegenthart[1]; [1]Groningen/NL, [2]Charleston/US, [3]Eindhoven/NL, [4]Charleston, SC/US
Keywords:	Ischaemia / Infarction, Experimental investigations, Balloon occlusion, CT-Quantitative, CT, Cardiac, Animal (veterinary) studies

Purpose

Coronary artery disease (CAD) can be ruled out with high sensitivity and negative predictive value by using Computed tomography angiography (CTA). However, in case of an intermediate stenosis, it is often difficult to determine hemodynamic significance, reflected in the lower specificity and positive predictive value of CTA.(1) Therefore, functional testing of hemodynamic significance is often required (2, 3). Myocardial perfusion reduction is typically the first sign in the ischaemic cascade. Quantification of myocardial perfusion defects could lead to faster and more accurate diagnosis of CAD.

Quantitative CT myocardial perfusion imaging has shown to increase diagnostic performance in several recent studies (7-13). However, there is as of yet limited information about the relationship between stenosis grade and CT myocardial perfusion parameters. The use of a controllable porcine heart model allows for determining the performance of CT myocardial perfusion imaging at investigator-controlled stenosis grades. The purpose of this study was to evaluate the relationship between fractional flow reserve (FFR)-controlled coronary artery stenosis grades and myocardial perfusion parameters derived from dynamic CT myocardial perfusion imaging in an *ex-vivo* porcine heart model, in order to develop a CT imaging biomarker for myocardial perfusion.

Methods and Materials

The hearts of six Dutch landrace hybrid pigs were obtained from the slaughterhouse. Protocols at the slaughterhouse and laboratory were in accordance with EC regulations 1069/2009 regarding the use of slaughterhouse animal material for diagnosis and research, supervised by the Dutch Government (Dutch Ministry of Agriculture, Nature and Food Quality), and approved by the associated legal authorities of animal welfare (Food and Consumer Product Safety Authority).

In this study, perfusion setup according to Langendorff was used (PhysioHeartÒ, LifeTec Group, Eindhoven, The Netherlands) (14,15). A centrifugal pump was used to pump porcine blood from the venous reservoir retrograde through the aorta to the heart (figure 1). Blood was pumped through the coronary arteries, preventing the aortic valve from opening. Blood was oxygenated and kept at a temperature of approximately 38°C. A mixture of glucose and insulin was added to keep the blood glucose level between 5 and 7 mmol/L. All hearts were defibrillated at 10 to 30 Joules in order to acquire stable sinus. An external pacemaker was used to stabilize the hearts, if necessary. Electrocardiography (ECG) leads were place on the platform, which provided excellent conduction of the ECG signal to the CT (figure 2). An inflatable cuff was placed around the proximal circumflex (Cx) artery, after dissecting the proximal Cx from the surrounding tissue. A pressure wire was placed inside the Cx artery, allowing monitoring of the stenosis grade during the experiment. The pressure wire allowed calculation of FFR by comparing pressure before and after the stenosis. CT myocardial perfusion parameters were studied at six FFR-based stenosis grades: no stenosis, FFR 0.8, FFR 0.7, FFR 0.6, FFR 0.5 and total occlusion. Heart rate, arterial blood flow (ml/min) and arterial blood pressure (mmHg) were monitored during the experiment.

A third generation dual source CT system (SOMATOM Force, Siemens Healthineers, Forchheim, Germany) was used to analyze perfusion of the porcine hearts. Dynamic CT myocardial perfusion imaging was performed at all FFR-based stenosis grades. Dynamic CT scans were performed in shuttle mode during end-systole, providing a scan z-range of 102 mm, covering the entire heart. Other acquisition parameters included tube voltage 70 kV, tube current time product 350 mAs per rotation, and rotation time of 250 ms. The inflow tube was looped through the field of view, allowing for calculation of an arterial input function. Myocardial enhancement returned to baseline by applying a 5-minute delay between each contrast-enhanced scan acquisition. An injection of 15 mL (contrast to saline ratio 35%/65%) of ioxaglate (Hexabrix, 320 mg/mL, Guerbet, Paris, France) at 3 mL/s was used for the dynamic CT scans. Injection site was 200 cm prior to the aortic annulus, allowing proper mixing of blood and contrast. Dynamic scans were started five seconds before the injection of the contrast.

Dynamic CT data were reconstructed with 3.0 mm slice thickness and 1.5 mm increment in the short-axis plane. Perfusion datasets were analysed using Volume Perfusion CT (VPCT) myocardium software (Siemens). Myocardial segments were drawn at basal, mid-ventricular and apical level using the American Heart Association (AHA) 17-segment model (16). The apex was excluded from the analysis, resulting in a total of 16 segments per scan. The myocardial segments were divided into two groups based on the vessel territory: 1. left anterior descending (LAD)/ right coronary artery (RCA) territory - non-ischaemic and 2. segments perfused by the Cx - ischaemic. The total occlusion scan was used to determine the Cx segments. VPCT myocardium software calculates myocardial blood flow and volume for every separate voxel based on the arterial input function and the signal increase in the myocardium. Mean values of myocardial blood flow (MBF) (mL/100mL/min) and myocardial blood volume (MBV) (mL/100mL) were calculated per myocardial segment. Median values of MBF and MBV were compared between 'non-ischaemic' segments with normal perfusion and 'ischaemic' segments perfused by the Cx artery. The comparison was performed for each stenosis grade (no stenosis, FFR 0.80, FFR 0.70, FFR 0.60 and FFR 0.50).

Images for this section:

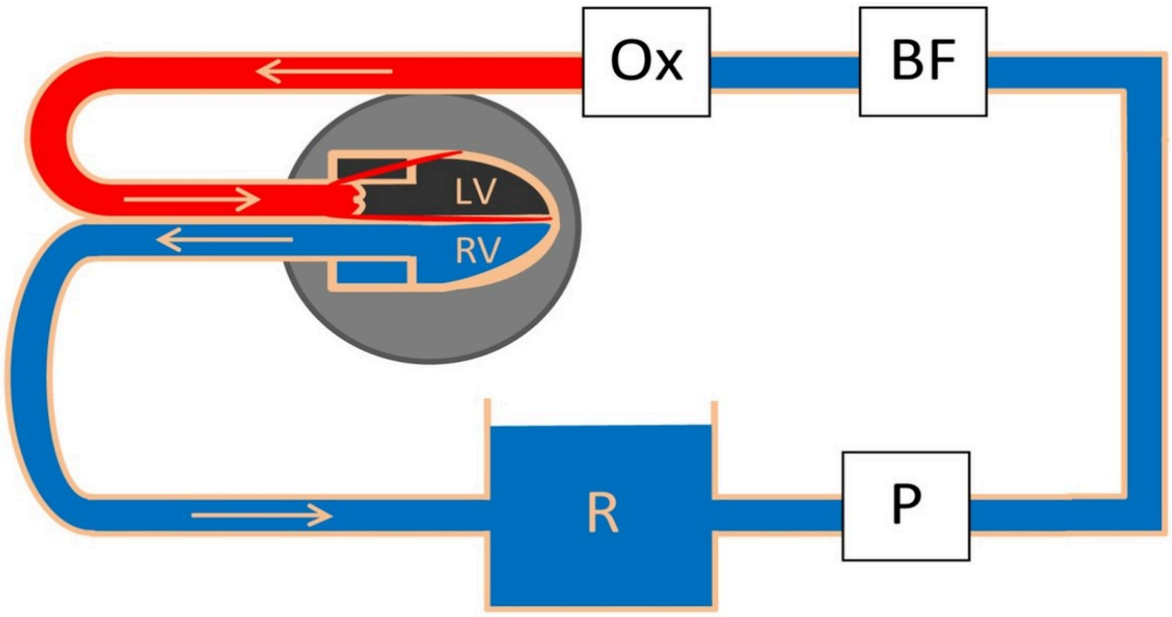

Fig. 1: Figure 1 Schematic representation of the Langendorff perfusion model. Blood flows from the pump (P) to the blood filter (BF) after which it is oxygenated and heated using an Oxygenator (Ox). Pressure is put on the aortic valve, and all blood traverses into the myocardium through the coronaries. Blood leaves the heart from the right ventricle and is collected in a large venous reservoir (R).

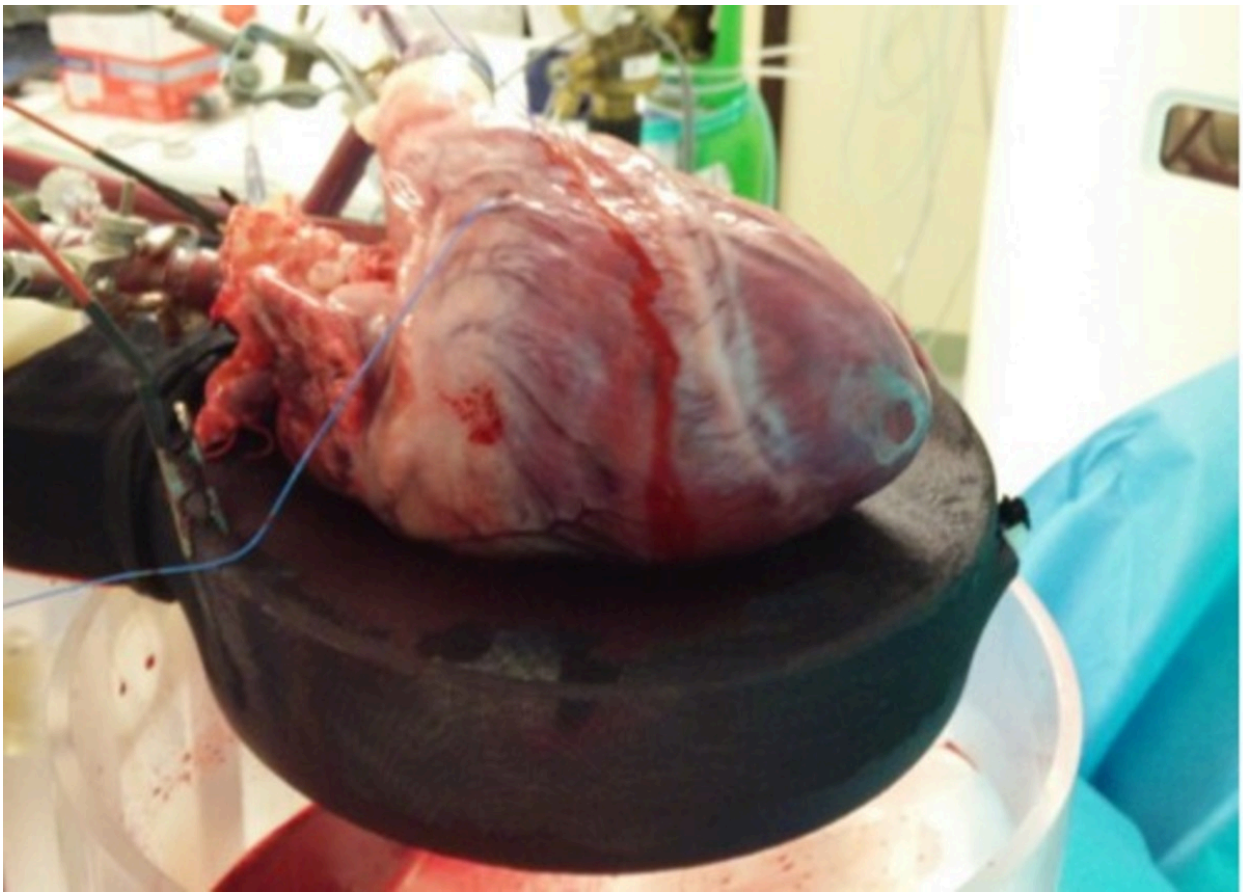

Fig. 2: Figure 2 The ex-vivo porcine heart set-up on the flexible cloth platform.

Results

All hearts recovered in stable sinus rhythm. In one case, a mechanical failure in the pressure wire prevented analysis of the pressure drop across the stenosis. Therefore, this heart was excluded from analysis. In five of the six hearts, all dynamic perfusion scans acquisitions were analysable. There were no significant artefacts that influenced image evaluation.

During the five successful experiments, arterial blood flow in the system ranged from 800 to 1210 mL/min with a mean value of 1021 mL/min and heart rate ranged from 83 to 115 beats per minute (bpm) with a median heart rate of 111 bpm. The mean arterial pressure ranged from 73 to 90 mmHg with a mean value of 81 mmHg.

80 (16 segments x 5 hearts) myocardial segments per stenosis grade (480 segments including all six stenosis grades) were analysed. 22 of 80 segments showed a perfusion defect, based on the total occlusion scan, resulting in a total of 132 ischaemic segments (6 stenosis grades x 22 segments) in the Cx territory. At FFR # 0.70, a significant difference in CT-determined MBF was found between ischaemic and non-ischaemic segments (Mann-Whitney-U-test, $p<0.05$) with a median MBF of 79 mL/100mL/min (IQR: 66-90) for non-ischaemic segments and 56 mL/100mL/min (IQR: 46-73) for ischaemic segments. For MBV, a significant difference between ischaemic and non-ischaemic segments was found at a FFR # 0.80 (Mann-Whitney-U-test, $p<0.05$) with median MBV values of 7.6 (IQR: 7.0-8.3) and 7.1 ml/100ml (IQR: 6.0-8.2) for the non-ischaemic and ischaemic myocardial segments, respectively.

Conclusion

In an *ex-vivo* Langendorff porcine heart experiment, differences in CT-derived myocardial perfusion parameters between ischaemic and non-ischaemic segments can be detected at stenosis grades with an FFR<0.80. This model can be used in the systematic development and study of new imaging biomarkers for myocardial perfusion in a highly controllable and adjustable environment for CT. Additional research in a clinical setting is required to translate the findings of this study into suitable cut-off values for quantitative CT perfusion parameters in patients with CAD.

References

1. Hulten EA, Carbonaro S, Petrillo SP, Mitchell JD, Villines TC. Prognostic value of cardiac computed tomography angiography: a systematic review and meta-analysis. J Am Coll Cardiol. 2011 Mar 8;57(10):1237-47.

2. Jaarsma C, Leiner T, Bekkers SC, Crijns HJ, Wildberger JE, Nagel E, et al. Diagnostic performance of noninvasive myocardial perfusion imaging using single-photon emission computed tomography, cardiac magnetic resonance, and positron emission tomography imaging for the detection of obstructive coronary artery disease: a meta-analysis. J Am Coll Cardiol. 2012 May 8;59(19):1719-28.

3. Takx RA, Blomberg BA, El Aidi H, Habets J, de Jong PA, Nagel E, et al. Diagnostic accuracy of stress myocardial perfusion imaging compared to invasive coronary angiography with fractional flow reserve meta-analysis. Circ Cardiovasc Imaging. 2015 Jan;8(1):10.1161/CIRCIMAGING.114.002666.

4. Rossi A, Merkus D, Klotz E, Mollet N, de Feyter PJ, Krestin GP. Stress Myocardial Perfusion: Imaging with Multidetector CT. Radiology. 2014 Jan;270(1):25-46.

5. Flohr TG, De Cecco CN, Schmidt B, Wang R, Schoepf UJ, Meinel FG. Computed tomographic assessment of coronary artery disease: state-of-the-art imaging techniques. Radiol Clin North Am. 2015 Mar;53(2):271-85.

6. Boiselle PM, Choe YH, Leipsic J, Pugliese F, Schoepf UJ, Vliegenthart R. Expert opinion: How and when to perform CT myocardial perfusion imaging. J Thorac Imaging. 2015 May;30(3):167-8.

7. Bamberg F, Marcus RP, Becker A, Hildebrandt K, Bauner K, Schwarz F, et al. Dynamic myocardial CT perfusion imaging for evaluation of myocardial ischemia as determined by MR imaging. JACC Cardiovasc Imaging. 2014 Mar;7(3):267-77.

8. Ho KT, Ong HY, Tan G, Yong QW. Dynamic CT myocardial perfusion measurements of resting and hyperaemic blood flow in low-risk subjects with 128-slice dual-source CT. Eur Heart J Cardiovasc Imaging. 2015 Mar;16(3):300-6.

9. Kono AK, Coenen A, Lubbers M, Kurata A, Rossi A, Dharampal A, et al. Relative myocardial blood flow by dynamic computed tomographic perfusion imaging predicts hemodynamic significance of coronary stenosis better than absolute blood flow. Invest Radiol. 2014 Dec;49(12):801-7.

10. Tanabe Y, Kido T, Uetani T, Kurata A, Kono T, Ogimoto A, et al. Differentiation of myocardial ischemia and infarction assessed by dynamic computed tomography perfusion imaging and comparison with cardiac magnetic resonance and single-photon emission computed tomography. Eur Radiol. 2016 Feb 6.

11. Wichmann JL, Meinel FG, Schoepf UJ, Lo GG, Choe YH, Wang Y, et al. Absolute Versus Relative Myocardial Blood Flow by Dynamic CT Myocardial Perfusion Imaging in Patients With Anatomic Coronary Artery Disease. AJR Am J Roentgenol. 2015 Jul;205(1):W67-72.

12. Wichmann JL, Meinel FG, Schoepf UJ, Varga-Szemes A, Muscogiuri G, Cannao PM, et al. Semiautomated Global Quantification of Left Ventricular Myocardial Perfusion at Stress Dynamic CT:: Diagnostic Accuracy for Detection of Territorial Myocardial Perfusion Deficits Compared to Visual Assessment. Acad Radiol. 2016 Apr;23(4):429-37.

13. Pelgrim GJ, Dorrius M, Xie X, den Dekker MA, Schoepf UJ, Henzler T, et al. The dream of a one-stop-shop: Meta-analysis on myocardial perfusion CT. Eur J Radiol. 2015 Jan 10.

14. Langendorff O. Untersuchungen am überlebenden Säugertierherzen. Plügers Arch. 1895;61:291-332.

15. de Hart J, de Weger A, van Tuijl S, Stijnen JM, van den Broek CN, Rutten MC, et al. An ex vivo platform to simulate cardiac physiology: a new dimension for therapy development and assessment. Int J Artif Organs. 2011 Jun;34(6):495-505.

16. Cerqueira MD, Weissman NJ, Dilsizian V, Jacobs AK, Kaul S, Laskey WK, et al. Standardized myocardial segmentation and nomenclature for tomographic imaging of the heart. A statement for healthcare professionals from the Cardiac Imaging Committee of the Council on Clinical Cardiology of the American Heart Association. Circulation. 2002 Jan 29;105(4):539-42.